

X-ray near-edge structure analysis of ZnSe, ZnMnSe and ZnFeSe: experimental and theoretical studies

This article has been downloaded from IOPscience. Please scroll down to see the full text article.

1994 J. Phys.: Condens. Matter 6 5771

(<http://iopscience.iop.org/0953-8984/6/29/019>)

View [the table of contents for this issue](#), or go to the [journal homepage](#) for more

Download details:

IP Address: 171.66.16.147

The article was downloaded on 12/05/2010 at 18:58

Please note that [terms and conditions apply](#).

X-ray near-edge structure analysis of ZnSe, ZnMnSe and ZnFeSe: experimental and theoretical studies

P M Lee†, A Kisiel‡, E Burattini§ and M Demianiuk¶

† School of Physics and Materials, Lancaster University, Lancaster LA1 4YB, UK

‡ Instytut Fizyki, Uniwersytet Jagiellonski, 30-059 Krakow, Reymonta 4, Poland

§ Istituto Nazionale di Fisica Nucleare, Laboratori Nazionali di Frascati, I-00044 Frascati, Italy

¶ Instytut Fizyki Technicznej, WAT, Warszawa, Poland

Received 21 February 1994, in final form 22 April 1994

Abstract. Experimental studies of x-ray absorption edges have been carried out in ZnSe, $\text{Zn}_{1-x}\text{Mn}_x\text{Se}$ ($x=0.05$ and 0.1) and $\text{Zn}_{1-x}\text{Fe}_x\text{Se}$ ($x=0.22$) for the K edges of Se, Zn, Mn and Fe. A comparison is made for a zincblende (ZB) crystalline structure of ZnSe, ZnMnSe and ZnFeSe with calculated results from electron densities of states in the conduction band of these materials obtained from a band calculation of the ferromagnetic phase of $\text{Zn}_{1-x}\text{Mn}_x\text{Se}$ ($x=0.5$) and $\text{Zn}_{1-x}\text{Fe}_x\text{Se}$ ($x=0.25$) using the LMTO method. The agreement between the theoretical x-ray absorption edges and experimental data is satisfactory. Further, a comparison based on the density of states for ferromagnetic and antiferromagnetic ordering has been carried out in the case of ZnFeSe. Using the virtual crystal model for ZnFeSe and ZnMnSe, the Se K edges of the hypothetical zincblende structure of FeSe and MnSe as well as a hybridized contribution of FeSe and MnSe in ZnFeSe and ZnMnSe have been extracted. Comparing the data with the conduction band of pure ZnSe, taken as a standard compound, these show a maximum of the p-like contribution in ZnFeSe situated at about 1.7 eV (maximum A) below, and 9.6 eV (maximum B) above, the corresponding energy of the conduction band minimum for ZnSe, and at about 0.65 eV below and 11.8 eV above it for ZnMnSe.

1. Introduction

ZnSe, $\text{Zn}_{1-x}\text{Fe}_x\text{Se}$ ($0 < x < 0.22$) and $\text{Zn}_{1-x}\text{Mn}_x\text{Se}$ ($0 < x < 0.15$) crystallizing in the zincblende structure possess many interesting semiconducting properties which have recently been increasingly studied. A band structure study of ZnSe has shown that this semiconducting compound is characterized by a large and direct energy gap [1]. Such theoretical band structure studies which have been made by the pseudo-potential method have been verified by optical as well as by photo-emission [2] and bremsstrahlung isochromat spectroscopy (BIS) [3] measurements. Recently, there have been more complete band structure calculations for pure ZnSe using self-consistent, relativistic LMTO methods [4]. These have been used to make a comparison with experimental optical and photoemission data using non-constant matrix elements of the optical transitions. The agreement between the experimental data and the theoretical single-particle calculations is found to be good [4]. In comparison with the well known band structure of pure ZnSe, the information about the band structure of the ZnSe ternary compounds with Mn and Fe is less well understood. ZnFeSe and ZnMnSe belong to a class of materials often referred to as dilute magnetic semiconductors (DMSs) since they exhibit properties that are unique from both the semiconducting and magnetic points of view [5]. Recently, II–VI DMSs have

attracted considerable attention as a result of the large exchange interaction between the band electrons and Fe d or Mn d ions, the so called sp-d super-exchange interaction [6, 7]. The Fe and Mn 3d states are split into two groups of sublevels by an exchange interaction (Slater splitting). In the tetrahedral crystalline field, the occupied spin-up states are localized in the valence band region similar to the case of CdFeSe; Fe ion occupied states also create in the gap so called 'deep donor' states [8, 9]. Data on the unoccupied spin-down states suggests that they are either located in the conduction band or are situated below the conduction band minimum [10, 11]. These 3d states can hybridize with Se as well as with cation s and p states so that a further distortion of the band structure and modification of the density of states (DOS) is likely to occur. The aim of this paper is to present the experimental XANES studies and LMTO theoretical analysis of the conduction bands for ZnMnSe and ZnFeSe and for comparison purposes those of pure ZnSe. These calculations consider a crystalline system rather than a random distribution of Fe or Mn and Zn atoms in the cation sublattice, but some general features of the results and an interpretation using the virtual crystal model allow us to compare these theoretical results with experiment. The effect of Fe or Mn on the conduction bands is not yet clear and to date can only be inferred from the recent fundamental reflectivity studies of ZnFeSe and ZnMnSe in a wide energy range from 1 to 30 eV [12]. The maximum contribution of Fe or Mn 3d unoccupied states to the conduction band of ZnFeSe or ZnMnSe, respectively, can be estimated from x-ray absorption analysis of the K edges. Also recent studies have shown that XANES for binary [13] and several ternary semiconducting compounds [14-17] can be described satisfactorily by a one electron approximation. Additionally [14-17] it has been shown that a virtual crystal model can be applied consistently to extract, from the experimental data for ZnFeSe and ZnMnSe, the x-ray absorption edges of the hypothetical zincblende structure, FeSe and MnSe. The layout of the paper is as follows: section 2 describes experimental details, experimental results and the method of interpreting the experimental data; in section 3 an outline of the theoretical calculations is presented; section 4 contains conclusions.

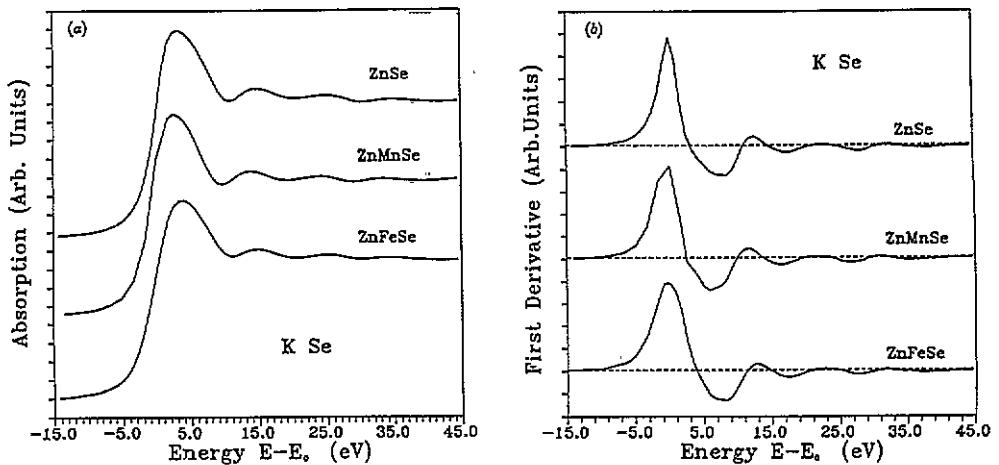


Figure 1. Experimental x-ray absorption Se K edges (a) and their first derivatives (b) for ZnSe, ZnMnSe and ZnFeSe.

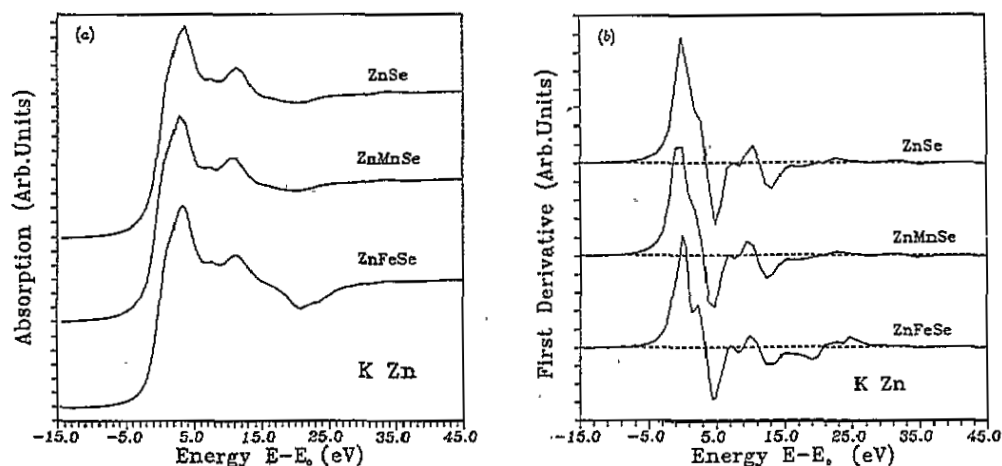


Figure 2. Experimental x-ray absorption Zn K edges (a) and their first derivatives (b) for ZnSe, ZnMnSe and ZnFeSe.

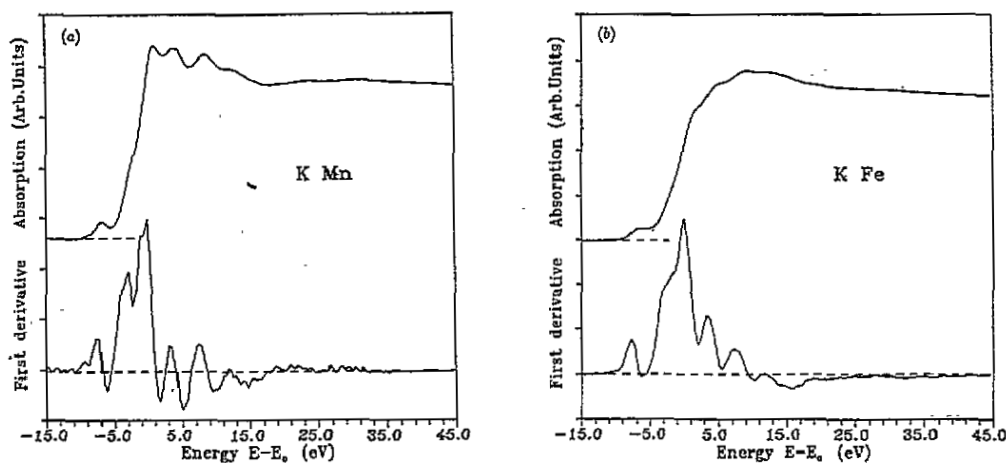


Figure 3. Experimental x-ray absorption for the Mn K edge and its first derivative for ZnMnSe (a) and the Fe K edge and its first derivative for ZnFeSe (b).

2. Experiment and results

X-ray absorption measurements have been carried out with the use of synchrotron radiation at the Adone Wiggler facility in Frascati utilizing the Si(111) and Si(220) channel-cut crystal monochromators [18]. The original samples were high-purity monocrystalline ZnSe, $Zn_{1-x}Mn_xSe$ ($x = 0.05$ and 0.1) and $Zn_{1-x}Fe_xSe$ ($x = 0.22$) produced by a high-pressure Bridgman method [19]. To obtain thin specimens of a controlled thickness and homogeneity as required by x-ray absorption techniques, the samples were finely powdered and deposited on polyacetate films. XAS measurements have been carried out on the Se as well as Zn and Fe K edges. The energy resolution of an experimental set-up of the type used by us is limited by the finite vertical divergence of the photon beam and the finite width of the rocking curve of the monochromating crystal. The resulting instrumental Gaussian broadening of the natural width of all measured edges has been estimated to be about 1.81

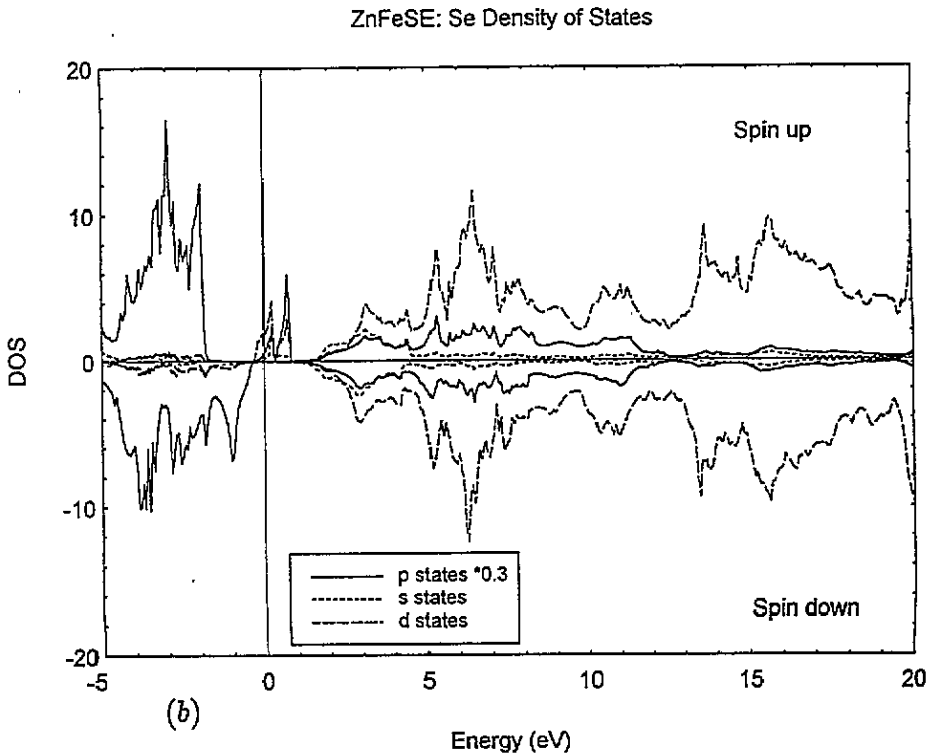
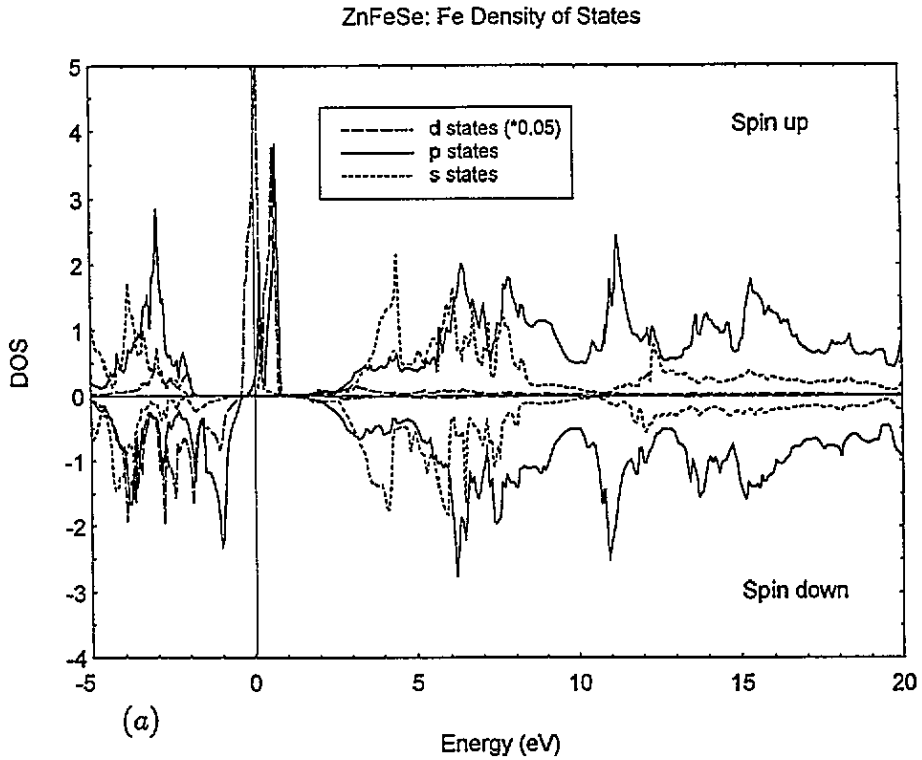


Figure 4. (Continued opposite.)

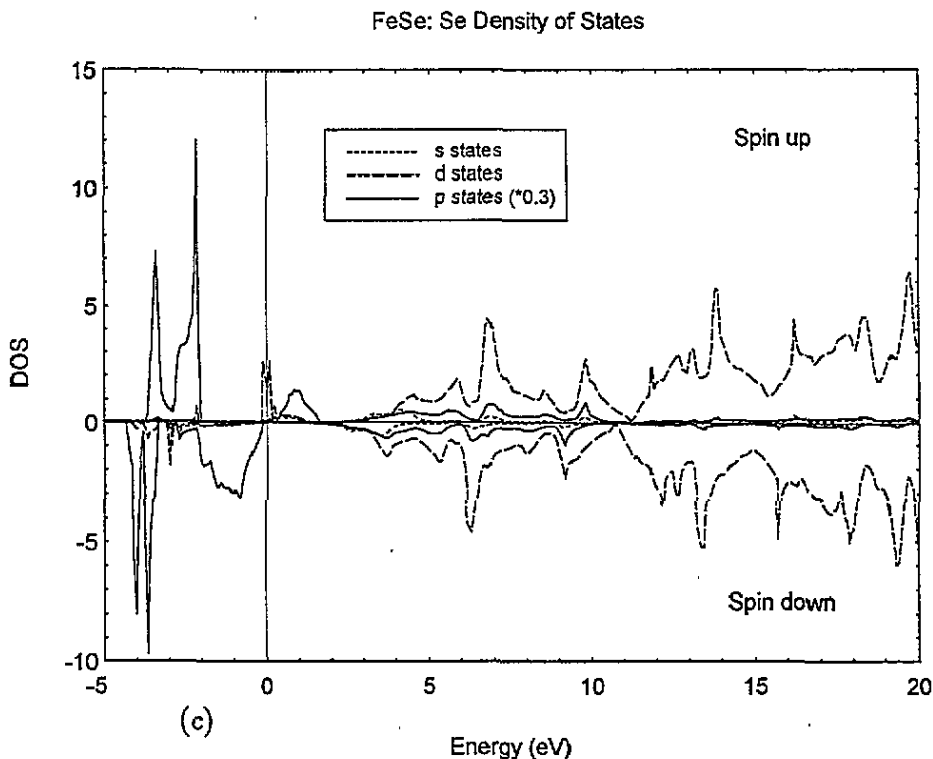


Figure 4. (Continued.) Density of states (DOS) for $\text{Zn}_{0.75}\text{Fe}_{0.25}\text{Se}$ around the (a) Fe and (b) Se atoms for the upper valence and lower conduction bands. 4(c) illustrates the same features for FeSe. The full line represents the p states, the dotted line the s states and the broken line the d states. Note that values for the d states in (a) and p states in (b) and (c) are scaled as indicated.

eV for Fe and 1.57 eV for Mn K edges and 2.04 eV for Zn and 2.44 eV for Se K edges. The contribution of each edge to the absorption coefficient has been isolated by extrapolating the pre-edge region to higher energies by a Victoreen-like fit and by subtracting the fitted curve from the remaining experimental spectrum [20]. Figure 1, figure 2 and figure 3 present the experimental data for Se, Zn and Fe or Mn K edges (after subtraction of the pre-edge contribution and normalization of the energy scale to the first inflection point at the edge) and their first derivatives for ZnSe, ZnFeSe and ZnMnSe. We have applied the procedure of the experimental data reduction reported earlier [14]. This approach provides a direct comparison of the experimental data with results derived from the projected density of states calculated in a limited energy range (up to cut-off energy ϵ). Table 1 contains values of all the parameters necessary for the experimental data reduction.

3. Calculated results

As previously [14, 15], calculations of the energy states in an ordered lattice have been used to obtain results for absorption coefficients to compare with the experimental data. These have been obtained for ZnSe, $\text{Zn}_{0.75}\text{Fe}_{0.25}\text{Se}$, $\text{Zn}_{0.5}\text{Fe}_{0.5}\text{Se}$, $\text{Zn}_{0.5}\text{Mn}_{0.5}\text{Se}$ and FeSe (zincblende structure). The LMTO method was used in the calculation of the energy levels and densities of states. The II-VI compounds (and the alloys considered here) have open structures which require empty spheres in addition to the atomic spheres for Zn, Fe, Mn and

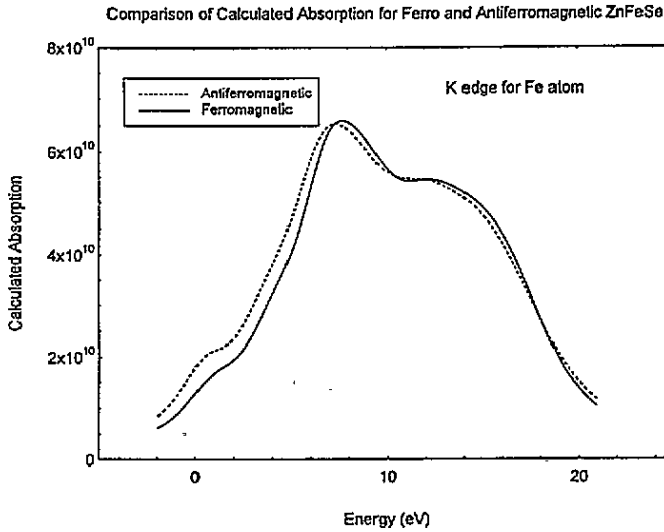


Figure 5. Comparison of the x-ray K edge for Fe calculated for the ferromagnetic and antiferromagnetic states of ZnFeSe with 50% content of Fe.

Table 1. Values of the lifetime parameters in eV used in calculating the absorption coefficient for a range of energies up to a cut-off value $\epsilon = 17$ eV.

	Γ_L (eV)	Γ_G (eV)	$\Delta\Gamma_\epsilon$ (eV)
Se	1.98	2.44	2.99
Zn	1.40	2.04	2.26
Fe	1.0	1.81	2.26
Mn	1.05	1.57	2.26

Se within the unit cell. For the ordered ternary alloys, a simple cubic cell was used with 16 atomic spheres in total consisting of eight atoms and eight empty spheres. For the 25% alloys a ferromagnetic structure was calculated but for the 50% case both ferromagnetic and antiferromagnetic cases were obtained. Using the angular-resolved density of states, $N_l(E)$ with $l = 0, 1, 2$, obtained from the calculations for the different species in the lattice, the absorption due to the electrons in the conduction bands can be calculated [14, 15]. In carrying out these calculations the matrix elements for the transitions are taken to be constant, independent of the energy. Lifetime and other effects are also treated similarly as before. The hybridization effects between the Fe d states and the states at the bottom of the conduction bands are an important feature in the alloys. This p-d hybridization gives rise to the states at the x-ray edge which are shown in the graphs of densities of states in figures 4(a), b and c. The position of such states on the energy scale is at $E = 0$ and the relevant peaks are shown in the p state contribution in both the Fe and Se cells at and just above $E = 0$ in the spin-up bands. Figures 4(a) and 4(b) illustrate this and present the DOS for ferromagnetic ZnFeSe around Fe and Se atoms in the energy range covering the top of the valence band and the lower conduction bands. Figure 4(c) shows the corresponding feature in FeSe. In all three figures, scaling of either d or p values has been used to indicate the full range on a single scale. In order to see the effect of ferromagnetic as opposed to antiferromagnetic

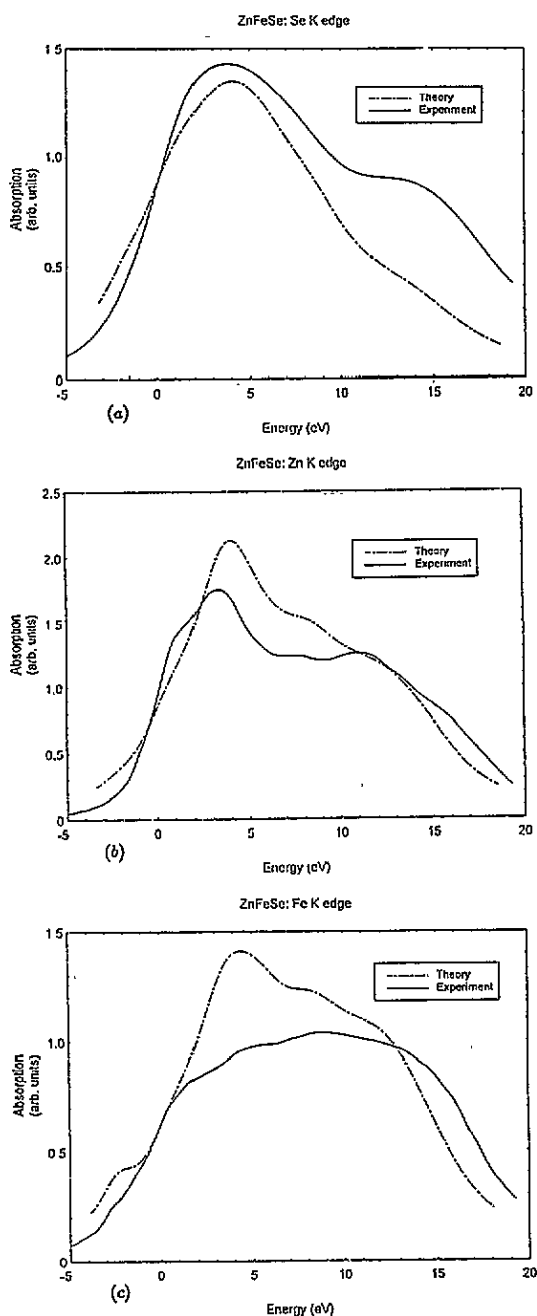


Figure 6. Comparison of the experimental (solid line) and theoretical (broken line) K edges of Se (a), Zn(b) and Fe(c) in ZnFeSe.

ordering on the calculated absorptions results for both cases for $\text{Zn}_{0.5}\text{Fe}_{0.5}\text{Se}$ are shown in figure 5. Differences expected because of the different positions in energy of the d states in the two cases are seen to be small.

Results comparing the calculated absorptions for ZnFeSe and ZnMnSe with experimental

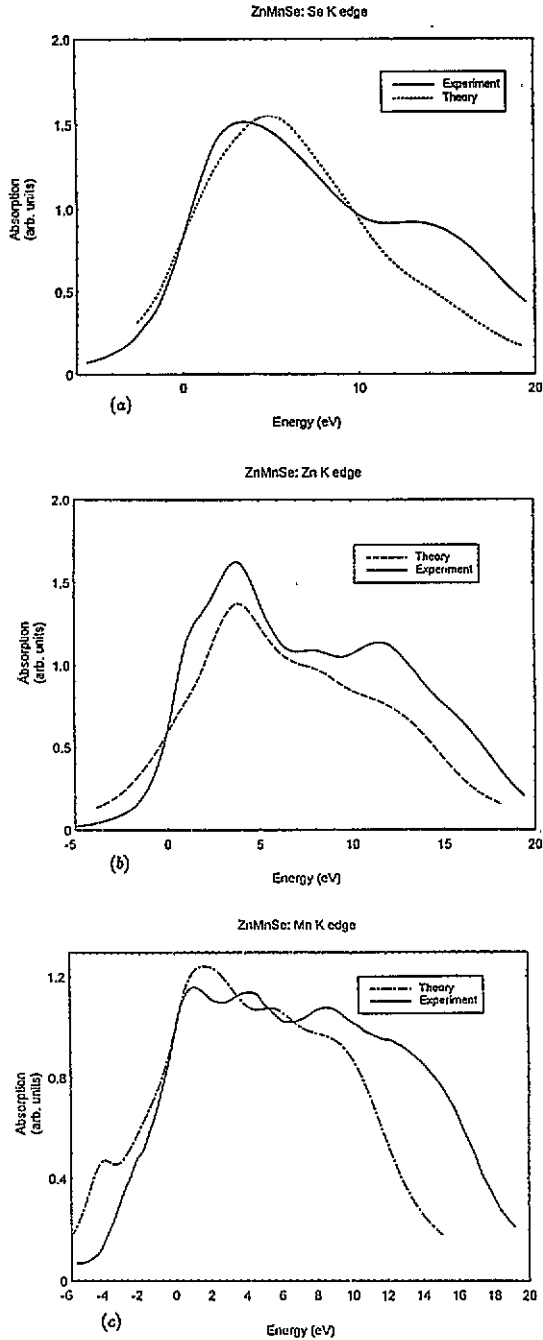


Figure 7. Comparison of the experimental (solid line) and theoretical (broken line) K edges for Se (a), Zn (b) and Mn (c) in ZnMnSe.

data, reduced to an energy cut-off 17 eV above the conduction band edge, are shown in figures 6 and 7. In including the lifetime effects in the calculations, the values of Γ used due to core hole lifetimes (Γ_L), instrumental width (Γ_G) and conduction band state lifetimes

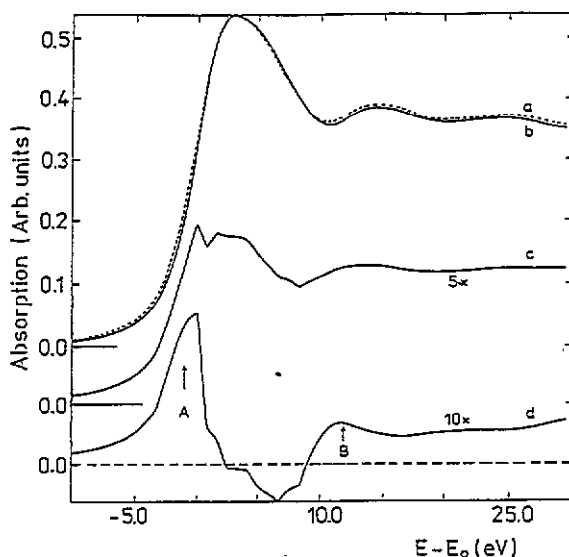


Figure 8. Virtual crystal model analysis of the experimental x-ray absorption Se K edges for ZnMnSe. Curve a (dotted line)—absorption coefficient for ZnMnSe on reduced energy scale, curve b—ZnSe for comparison, curve c—absorption edge of the hypothetical zincblende MnSe extracted with use of the virtual crystal model, curve d—a contribution of the hybridized Mn 3d and 4s electronic states in ZnMnSe.

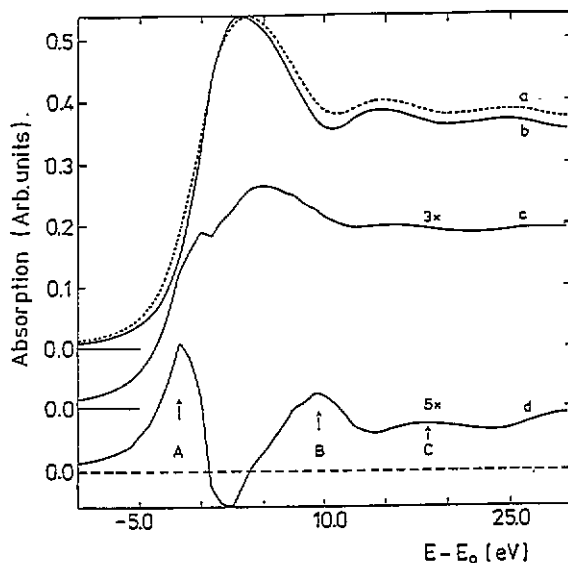


Figure 9. Virtual crystal model analysis of the experimental x-ray absorption Se K edges for ZnFeSe. Curve a (dotted line)—absorption coefficient for ZnFeSe on reduced energy scale, curve b—ZnSe for comparison, curve c—absorption edge of the hypothetical zincblende FeSe extracted with use of the virtual crystal model, curve d—a contribution of the hybridized Fe 3d and 4s electronic states in ZnFeSe.

($\Delta\Gamma_\epsilon$) are given in table 1. The sources of these values are given in [14]. Normalization of the two sets of data is achieved by matching the calculated results to the experimental data

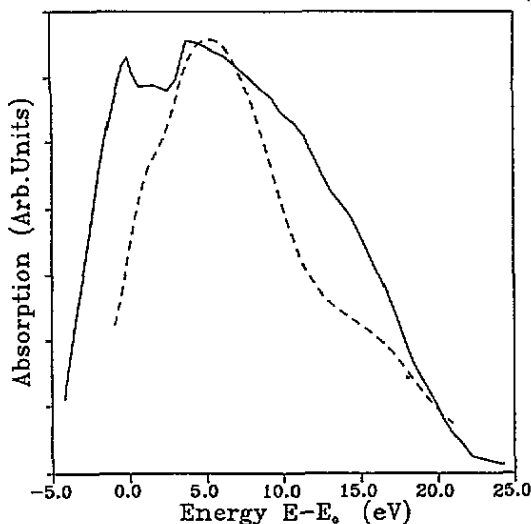


Figure 10. Comparison of the calculated K edge for Se for the hypothetical zincblende FeSe, dashed line, with that extracted from reduced experimental data (solid line).

at the energy where the maximum value of the derivative with respect to energy occurs in both cases. The zero of the energy scale is then moved to that point.

The K absorption for Fe, as calculated, relies entirely on the p state density in the atomic sphere around the Fe atom at energies close to the bottom of the conduction band. This in turn derives very much from the hybridization between Fe and Se atoms, with additional influence from the Zn atom. This p-d hybridization gives a peak in the DOS matching the peak in the p state DOS of the Fe atom as seen in figure 4(a). This shows up in the absorption as a small feature in the leading edge. This small feature exists also in the Se (see figures 4(b) and 6) and Zn calculated edges since the p-d hybridization effect works both ways as indicated above. Using both the experimental data and the calculated values we can apply a virtual crystal model in the form of the equation

$$\text{Zn}_{1-x}\text{Fe}_x\text{Se}_{1-x} = x\text{FeSe}$$

to determine the properties of the x-ray absorption edge of zincblende FeSe.

This has been done for $x = 0.22$ for the calculated case of the Se edge to extract a result and compare it with the one directly calculated for $x = 0.25$. The result shown in figures 8 and 9 indicates an enhancement of the feature mentioned due to the contribution of the Zn hybridization. Figure 10 shows a comparison of the calculated K Se absorption edge of hypothetical zincblende FeSe with the corresponding absorption edge of FeSe extracted from the experimental data using the virtual crystal model. The two curves in figure 10 are similar and both show features at about 0.0, 5.0 and 15.0 eV. The rather broader shape of the experimental curve arises from the greater errors implicit in the extraction process.

4. Conclusions

A XANES analysis shows that the x-ray absorption edges of ZnSe, ZnMnSe and ZnFeSe differ significantly. A comparison of the experimental data with calculated values based on theoretical LMTO band structures shows satisfactory agreement, particularly in the position

of the main maxima of the experimental spectra. In addition, results for the calculated Fe absorption edges with ferromagnetic and antiferromagnetic ordering of spins localized on Fe do not differ significantly in comparison with the experimental data, and therefore either may be used in the comparison of the data. A hypothetical zincblende FeSe obtained from experimental data by use of the virtual crystal model also shows good agreement with calculated zincblende FeSe. A maximum contribution of the Fe 4s and 3d hybridized states in ZnFeSe can be identified at about 1.7 eV below the conduction band minimum and also at 9.6 eV above this minimum. For ZnMnSe maximum contributions of the Mn 3d and 4s hybridized states are found at about 0.65 eV below the conduction band minimum and 11.8 eV above it.

Acknowledgments

We wish to thank Ewa Czarnecka-Such for technical assistance during the preparation of this paper. Also we would like to thank P Fornasini, Department of Physics, Trento University, for providing computer programs used in the processing of the experimental data. Finally thanks are due to the technical staff of the PWA group of the Laboratori Nazionale di Frascati for their help and hospitality. This work is in part supported by programme No PB-2528/2/91 and 7 F201 042 06 of the Polish Committee for Scientific Research.

References

- [1] *Landolt-Bornstein New Series* 1982 vol 17 ed K H Hellwege (Berlin: Springer) p 126
- [2] Ley L, Kowalczyk S, Pollak R and Shirley D 1972 *Phys. Rev. Lett.* **29** 1088
Ley L, Pollak R, McFeely F R, Kowalczyk S and Shirley D 1974 *Phys. Rev. B* **9** 600 and references therein
- [3] Chelikowski J R, Wagener T J, Weaver J H and Jin A 1989 *Phys. Rev. B* **40** 9644
- [4] Markowski R, Piacentini M, Debowska D, Zimnal-Starnawska M, Lama F, Zema N and Kisiel A 1994 *J. Phys.: Condens. Matter* **6** 3207
- [5] Furdyna J K 1982 *J. Appl. Phys.* **53** 7637
Ramdas A K 1982 *J. Appl. Phys.* **53** 7649
- [6] Weidemann R, Gumlich H E, Kupsch M, Middelmann U and Becker U 1992 *Phys. Rev. B* **45** 1172
- [7] Twardowski A, Glod P, de Jonge W J M and Demianiuk M 1987 *Solid State Commun.* **64** 63
- [8] Mycielski A, Dzwonkowski P, Kowalski B, Orlowski B A, Dobrowolska M, Arciszewska A, Dobrowolski W and Baranowski J M 1986 *J. Phys. C: Solid State Phys.* **19** 3605
- [9] Mycielski A 1988 *Acta Phys. Pol. A* **73** 839
- [10] Kisiel A, Piacentini M, Antonangeli F, Zema N and Mycielski A 1989 *Solid State Commun.* **70** 693
- [11] Konior J, Kisiel A, Oleszkiewicz J, Kaprzyk S and Burattini E 1994 *Solid State Commun.* submitted
- [12] Zimnal-Starnawska M, Debowska D, Piacentini M and Kisiel A private communication
- [13] Kisiel A, Dalba G, Fornasini P, Podgorny M, Oleszkiewicz J, Rocca F and Burattini E 1989 *Phys. Rev. B* **39** 7895
- [14] Kisiel A, Ali Dahr A-I, Lee P M, Dalba G, Fornasini P and Burattini E 1990 *Phys. Rev. B* **42** 11 114
- [15] Kisiel A, Ali Dahr A-I, Lee P M, Dalba G, Fornasini P and Burattini E 1991 *Phys. Rev. B* **44** 11 075
- [16] Kisiel A, Lee P M, Burattini E, Dalba G, Fornasini P and Giriat W 1992 *Solid State Commun.* **81** 151
- [17] Burattini E, Kisiel A, Markowski R, Dalba G and Giriat W 1993 *Acta Phys. Pol. A* **83** 10
- [18] Burattini E, Bernieri E, Balerna A, Mencuccini C, Rinzivillo R, Dalba G and Fornasini P 1986 *Nucl. Instrum. Methods A* **246** 125
- [19] Demianiuk M 1990 *Mater. Res. Bull.* **25** 337
- [20] Teo B K 1986 *EXAFS: Basic Principles and Data Analysis* (Berlin: Springer)